

Thermal behaviour of the $\text{NaYF}_4:\text{Yb}^{3+},\text{R}^{3+}$ materials

Tero Laihinen · Mika Lastusaari · Laura Pihlgren ·
Lucas C. V. Rodrigues · Jorma Hölsä

Received: 24 October 2014 / Accepted: 25 February 2015 / Published online: 25 March 2015
© Akadémiai Kiadó, Budapest, Hungary 2015

Abstract The $\text{NaYF}_4:\text{Yb}^{3+},\text{R}^{3+}$ (R: none, Pr, Nd, Sm, Eu, Tb or Dy) materials were prepared with selected dopant concentrations, using co-precipitation synthesis, to study the effect of the dopant and its concentration on the structure of these materials. The thermal behaviour of the as-prepared materials was studied with differential scanning calorimetry (DSC) and thermogravimetry. The structures prior to and after annealing were identified with X-ray powder diffraction. The materials were mainly hexagonal with occasional slight cubic impurity. The DSC curves revealed the cubic-to-hexagonal phase transition at

400–450 °C which temperature changes irregularly with the R^{3+} dopant and its concentration. The specific enthalpy of this transition varies also in a complicated way but may be correlated with the completeness of the transition. The hexagonal-to-cubic transition temperature (ca. 670 °C) is rather constant regardless of the R^{3+} dopant or its concentration. The temperatures and specific enthalpies of the phase transitions are useful when choosing the optimum dopant concentrations. It is also possible to estimate the structure prior to annealing with significant savings in use of resources. Only with Sm^{3+} and Dy^{3+} doping, no visible up-conversion luminescence was observed—in addition to the Er^{3+} and Tm^{3+} impurity emission. Eventually, it was found that the hexagonal form gives much stronger up-conversion luminescence and changes in the rare earth concentration allows the formation of this form.

T. Laihinen (✉) · M. Lastusaari · L. Pihlgren ·
L. C. V. Rodrigues · J. Hölsä
Department of Chemistry, University of Turku, FI-20014 Turku,
Finland
e-mail: telaih@utu.fi

M. Lastusaari
e-mail: miklas@utu.fi

L. Pihlgren
e-mail: laerle@utu.fi

L. C. V. Rodrigues
e-mail: lucascvr@iq.usp.br

J. Hölsä
e-mail: jholasa@utu.fi

T. Laihinen · L. Pihlgren
Doctoral Programme in Physical and Chemical Sciences,
University of Turku Graduate School (UTUGS),
FI-20014 Turku, Finland

M. Lastusaari · J. Hölsä
Turku University Centre for Materials and Surfaces (MatSurf),
Turku, Finland

L. C. V. Rodrigues · J. Hölsä
Instituto de Química, Universidade de São Paulo, São Paulo-SP,
Brazil

Keywords NaRF_4 · R^{3+} doping · Phase transitions ·
DSC · TG

Introduction

In up-conversion luminescence, absorption of two or more low-energy photons is followed by emission of a high-energy photon [1]. This phenomenon allows the conversion of NIR radiation usually to visible but nowadays increasingly also to NIR or UV radiation. Up-conversion luminescence can be useful in applications such as enhancement of photosynthesis [2], solar cells [3] and medical imaging [4]. In the two former applications, up-conversion luminescence materials can be used to convert otherwise unusable radiation to visible and thus to enhance the overall efficiency. In medical imaging, the up-converting materials enable NIR excitation, which is not absorbed by blood or tissues.

Interference from autoluminescence and tissue damage are then generally avoided. A key aspect of up-conversion luminescence materials in all applications is obviously strong luminescence, and also nanoscale size is required in, e.g. medical imaging. Unfortunately, up-conversion luminescence is still rather weak for materials in nanoscale. It is thus important to enhance the performance of the materials to achieve as strong up-conversion luminescence as possible.

NaYF_4 has been recognized as one of the most feasible hosts for efficient up-conversion luminescence [5–7]. The NaRF_4 (R: e.g. Y, Yb and Er) materials have three different structures [8, 9]: low-temperature (LT) cubic (α - NaRF_4 ; $\text{Fm}\bar{3}\text{m}$ (#225), Z: 2 [10]), hexagonal (β - NaRF_4 ; $\text{P6}_3/\text{m}$ (#176), Z: 1.5 [5, 10]) and high-temperature (HT) cubic, whose structure lacks detailed characterization. The hexagonal β form is the best for up-conversion luminescence [5–7]; therefore, the materials should be obtained in this form. This is achieved by heating the cubic α form at a temperature between the cubic-to-hexagonal (α - to β - NaRF_4) and hexagonal-to-HT cubic phase transitions, which occur around 400 and 700 °C, respectively. Both phase transitions are irreversible [11], and after cooling, all three structures can be quenched to room temperature.

Up-conversion luminescence has been observed from several rare earths (R: Pr [12], Nd [13], Sm [14], Eu [15], Tb [16], Dy [17], Ho [18], Er [5–7, 19, 20] and Tm [5, 20]). With the NaYF_4 host, the hexagonal structure yields the strongest luminescence [5–7]. The goal is thus to have as small nanomaterials with as strong luminescence as possible. Naturally, the annealing temperatures should then be kept as low as possible to achieve this trade-off. In this work, $\text{NaYF}_4:\text{Yb}^{3+},\text{R}^{3+}$ (R: none, Pr, Nd, Sm, Eu, Tb or Dy) materials were studied to determine the optimum annealing temperature as a function of dopant and its concentration. Finally, a relationship between the thermal behaviour of the material and the structure was established. The structure and phase purity of the as-prepared and post-annealed materials were analysed with X-ray powder diffraction (XPD). The thermal behaviour of the as-prepared materials was studied with differential scanning calorimetry (DSC) and thermogravimetry (TG). The ambient up-conversion luminescence of the post-annealed materials was routinely verified with NIR laser excitation at 976 nm at room temperature.

Materials and methods

Materials preparation

The $\text{NaYF}_4:\text{Yb}^{3+},\text{R}^{3+}$ (R: none, Pr, Nd, Sm, Eu, Tb or Dy) materials were prepared with selected dopant concentrations (x_{Yb} : 0.01–0.20 and x_{R} : 0.001–0.04) using co-precipitation

[19]. This involved the dissolution of solid NaF to distilled water, which was further mixed with aqueous solution of mixed YCl_3 , YbCl_3 and RCl_3 to obtain the stoichiometry desired. A Na/R ratio of 12.5 was used to force the formation of the NaRF_4 phase instead of the RF_3 one. After stirring for 1 h at room temperature, the precipitate thus formed was centrifuged (3766g) and washed thrice with water and once with ethanol. Each washing was followed by centrifuging. The precipitate was then dried in a vacuum desiccator at room temperature. Based on the DSC results, β form was obtained with annealing at 500 °C for 5 h in a static $\text{N}_2 + 10\% \text{H}_2$ gas sphere (the annealing temperature of 500 °C was considered sufficient to obtain the β - NaRF_4). After annealing, the materials were cooled down freely to the room temperature under the same gas sphere. More $\text{N}_2 + 10\% \text{H}_2$ gas was added to the quartz reactor during the cooling to prevent replacement air to enter.

Characterization

The structure and phase purity of the materials were analysed with the XPD measurements. The patterns were collected at room temperature with a Huber G670 image plate Guinier camera (2θ range 4–100°, data interval 0.005°) with monochromatic copper $\text{K}_{\alpha 1}$ radiation (λ : 1.54056 Å). The asymmetry of the reflections at low angles is due to the apparatus used. Even for Rietveld structure refinements, this effect can still be corrected with success, however.

The thermal behaviour of the as-prepared materials was studied with a TA Instruments SDT Q600 simultaneous TGA-DSC apparatus between 25 and 720 °C in flowing N_2 (flow rate: 100 $\text{cm}^3 \text{min}^{-1}$). A heating rate of 5 °C min^{-1} and sample mass of ca. 10 mg were used. The sample pan was made of aluminium oxide, and a similar but empty pan was used as the reference material. The specific enthalpies of the phase transitions were calculated by integration of the corresponding DSC signal area.

The up-conversion luminescence spectra of the materials inside a rotating capillary tube were measured at room temperature with an Ocean Optics PC2000-CCD spectrometer. The NIR excitation (λ_{exc} : 976 nm) source was a Hamamatsu L9418-04 NIR laser diode. Optical long- and short-pass filters were used before and after the sample, respectively. The emission was guided to the spectrometer with an optical fibre.

Results and discussion

Structure and phase purity

The as-prepared as well as post-annealed (for 5 h @ 500 °C) $\text{NaYF}_4:\text{Yb}^{3+},\text{R}^{3+}$ (R: Pr, Nd, Sm, Eu, Tb, Dy or

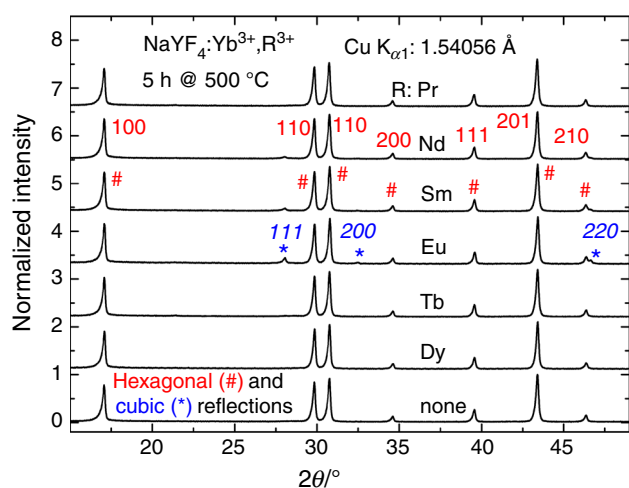


Fig. 1 XPD patterns of the annealed NaYF₄:Yb³⁺,R³⁺ (R: Pr, Nd, Sm, Eu, Tb, Dy or none) materials with approximately the same dopant concentrations (x_{Yb} : 0.20 and x_R : 0.02; x_{Yb} : 0.19 and x_{Pr} : 0.01)

none) have cubic and hexagonal structures, respectively, as revealed by the XPD measurements. Very slight amounts of the cubic form (Fig. 1) were also observed with the following annealed R³⁺ doped materials: Yb³⁺ only: x_{Yb} : 0.10 or 0.15, Yb³⁺,Sm³⁺: x_{Yb} : 0.20 and x_{Sm} : 0.02, Yb³⁺,Nd³⁺: x_{Nd} : 0.002 or 0.02, Yb³⁺,Eu³⁺: x_{Eu} : 0.002 or 0.02 and Yb³⁺,Tb³⁺: x_{Tb} : 0.04 or x_{Yb} : 0.10. For these materials, the exothermic α - β DSC signal was at higher temperature and also weaker than for the pure hexagonal ones; this will be discussed in more detail in the next chapter. Other impurities, e.g. crystalline NaF, were not observed. However, there might be amorphous NaF present since its presence has proven to be crucial to the formation of the hexagonal structure [21].

Thermal behaviour

The DSC curves of all NaYF₄:Yb³⁺,R³⁺ revealed both an exothermic signal between ca. 400 and 450 °C and an endothermic one at ca. 670 °C (Fig. 2) due to the formation of the β and HT cubic phase of NaYF₄:Yb³⁺,R³⁺, respectively. At least the α - to β -NaRF₄ phase transition is irreversible (see the end of the chapter). In general, the temperature of this transition seems to decrease with decreasing R³⁺ dopant size. However, the temperature differences are not very large; the largest difference is 5 °C when the dopant concentration is the same: x_R : 0.02 (R: Nd, Sm, Eu, Tb or Dy). Along with the concentration of the same R³⁺ dopant, the α - to β -NaRF₄ transition temperature and its variation behave more irregularly than with different R³⁺ dopants. For instance, with Tb³⁺ doping, the largest difference is 18 °C (x_{Tb} : 0.005–0.04 and x_{Yb} : 0.20; Fig. 3). In contrast, the hexagonal-to-HT cubic

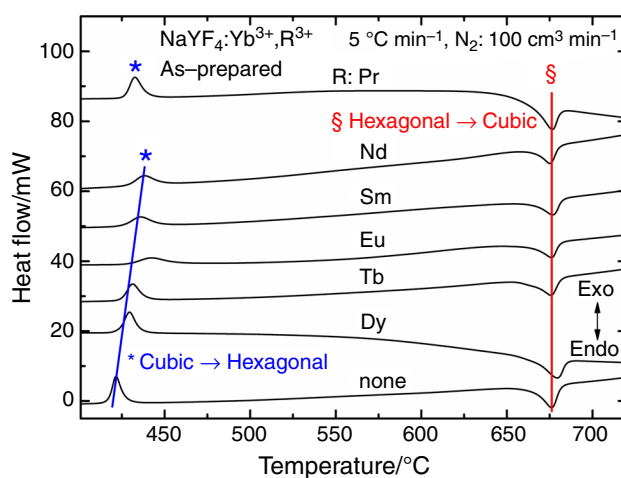


Fig. 2 DSC curves of the NaYF₄:Yb³⁺,R³⁺ (R: Pr, Nd, Sm, Eu, Tb, Dy or none) materials with approximately the same dopant concentrations (x_{Yb} : 0.20 and x_R : 0.02; x_{Yb} : 0.19 and x_{Pr} : 0.01)

phase transition temperature is rather constant regardless of the R³⁺ dopant and its concentration (Figs. 2, 3; Table 1). No clear reason was found for this difference (magnitude of variation) between the α - to β -NaRF₄ and hexagonal-to-HT cubic transition temperatures. However, the stoichiometry and structure of β -NaRF₄ are more well defined than those of α -NaRF₄, so the hexagonal-to-HT cubic phase transition involves lesser and less varied changes than the α - to β -NaRF₄ transition.

With the NaYF₄:Yb³⁺ materials, the α - to β -NaRF₄ transition temperature increases and the hexagonal-to-HT cubic one decreases with decreasing Yb³⁺ concentration (Table 1). At the same time, the specific enthalpy of both signals becomes substantially lower; this implies that the former transition is incomplete. This conclusion was confirmed by the XPD measurements; the pure hexagonal form (without any cubic) was obtained only with the highest

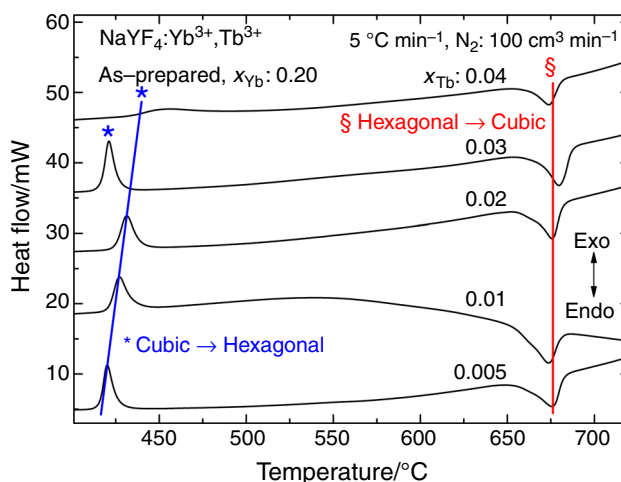


Fig. 3 DSC curves of the NaYF₄:Yb³⁺,Tb³⁺ materials as a function of the Tb³⁺ concentration

Table 1 Dopant concentrations, phase transition temperatures and specific enthalpies of the phase transitions of the $\text{NaYF}_4:\text{Yb}^{3+},\text{R}^{3+}$ (R: Pr, Nd, Sm, Eu, Tb, Dy or none) materials

x_{R}							Cubic \rightarrow hexagonal		Hexagonal \rightarrow cubic		I_{111} (cubic)/ I_{110} (hexagonal)
Yb	Pr	Nd	Sm	Eu	Tb	Dy	$T/^\circ\text{C}$	$\Delta H/J \text{ g}^{-1}$	$T/^\circ\text{C}$	$\Delta H/J \text{ g}^{-1}$	
0.10							480	0	660	32	1.33
0.15							435	26	664	52	0.36
0.20							417	71	665	100	0
0.01							419	72	684	100	0
0.05	0.001						427	58	679	83	0.03
0.10							419	72	664	126	0
0.01							427	71	677	104	0
0.10	0.01						428	63	676	90	0.03
0.19							427	68	665	96	0
		0.002					435	34	662	57	0.23
0.20		0.02					429	51	665	72	0.04
		0.03					429	62	666	86	0
		0.04					431	59	664	83	0
0.20			0.002				422	61	665	82	0
			0.02				426	48	665	72	0.06
				0.002			431	33	660	65	0.25
0.20				0.02			429	41	663	75	0.13
				0.03			421	66	666	91	0
				0.04			421	60	668	94	0
0.10					0.03		438	17	668	48	0.52
0.15							418	68	667	101	0
					0.005		416	69	658	104	0
0.20					0.01		421	70	657	102	0
					0.02		425	67	663	94	0
					0.03		417	68	667	99	0
					0.04		434	34	661	54	0.46
0.20						0.002	416	70	667	100	0
						0.02	424	71	667	97	0

Yb^{3+} concentration (when annealed at 500 °C). However, the Yb^{3+} concentration has a very weak effect on the α - to β - NaRF_4 transition temperature of the $\text{NaYF}_4:\text{Yb}^{3+},\text{Pr}^{3+}$ materials. The reason for this inconsistency is still unclear, and further studies are needed to elucidate this observation. The hexagonal-to-HT cubic transition temperature of the Pr^{3+} -doped materials decreases notably with increasing Yb^{3+} concentration.

With the $\text{NaYF}_4:\text{Yb}^{3+},\text{Nd}^{3+}$ materials, the α - to β - NaRF_4 transition temperature attained the lowest limit with $x_{\text{Nd}}: 0.03$, but the difference to the highest temperature was only 6 °C ($x_{\text{Nd}}: 0.002$; Table 1). This suggests that 3 % is

the optimum concentration of Nd^{3+} in $\text{NaYF}_4:\text{Yb}^{3+},\text{Nd}^{3+}$, when considering the structure alone and not the up-conversion luminescence. The hexagonal-to-HT cubic transition temperature behaves in the opposite way; it is the highest when $x_{\text{Nd}}: 0.03$ and the lowest when $x_{\text{Nd}}: 0.002$. Again the difference is small, only 4 °C. The specific enthalpies yielded similar results and the highest values were observed when $x_{\text{Nd}}: 0.03$. These observations also supported the XPD measurements; the cubic form was observed when $x_{\text{Nd}}: 0.002$ or 0.02. In general, it was interesting to find an optimum concentration at all since the difference between the ionic radius of Y and Nd is rather

large, which suggests that the stability of $\beta\text{-NaRF}_4$ would be the highest for the lowest dopant concentrations. A good example in this context is the much used laser material, Nd^{3+} -doped $\text{Y}_3\text{Al}_5\text{O}_{12}$ ($\text{Nd}:\text{YAG}$) [22].

The α - to $\beta\text{-NaRF}_4$ transition temperatures of the Sm^{3+} and Dy^{3+} -doped materials rise with the R^{3+} concentration (Table 1). However, the differences are quite small: only 4 and 8 °C, respectively. The hexagonal-to-HT cubic phase transition temperature is the same with both concentrations (the same R^{3+}). The specific enthalpies of both transitions were smaller for the higher Sm^{3+} concentration; with Dy^{3+} doping, these were almost the same.

With Eu^{3+} doping, the α - to $\beta\text{-NaRF}_4$ and hexagonal-to-HT cubic transition temperatures increase and decrease with decreasing Eu^{3+} concentration, respectively (Table 1). For the europium concentrations 0.03 or 0.04, the α - to $\beta\text{-NaRF}_4$ transition temperature is the same and the specific enthalpies are notably higher than for materials with lower concentrations, suggesting that the dopant concentration may be close to optimal. As expected, also these observations support the XPD measurements where the cubic form was observed when x_{Eu} was 0.002 or 0.02.

The transition temperatures of the $\text{NaYF}_4:\text{Yb}^{3+},\text{Tb}^{3+}$ materials vary irregularly when the Yb^{3+} concentration is constant ($x_{\text{Yb}}: 0.20$; Fig. 3). When $x_{\text{Tb}}: 0.04$, the specific enthalpy of the α - to $\beta\text{-NaRF}_4$ transition signal is significantly weaker and temperature is higher than with other dopant concentrations (Table 1). With constant Tb^{3+} concentration ($x_{\text{Tb}}: 0.03$), the α - β transition signal was at a radically higher temperature than with other Yb^{3+} concentrations, and the specific enthalpies of both signals were much lower with the lowest Yb^{3+} concentration ($x_{\text{Yb}}: 0.10$). These two materials ($x_{\text{Yb}}: 0.20 + x_{\text{Tb}}: 0.04$ and $x_{\text{Yb}}: 0.10 + x_{\text{Tb}}: 0.03$) were the only ones with the cubic form present.

Based on the DSC results, the specific enthalpies of the α - β transition of the $\text{NaYF}_4:\text{Yb}^{3+},\text{R}^{3+}$ materials were

eventually correlated with the intensity ratio between the XPD reflections 111 and 110 for the α - and $\beta\text{-NaRF}_4$ forms, respectively (Fig. 4). The following correlation between the amount of the cubic form and the specific enthalpy of the *cubic-to-hexagonal* transition is tentatively suggested: the larger is the specific enthalpy, less cubic form is present as well. This enables the estimation of the amount of the cubic form using the specific enthalpy measured with DSC. So far, the cubic form has not been obtained if the specific enthalpy is $>65 \text{ J g}^{-1}$. Annealing and XPD measurements are thus not necessary to identify which materials would contain cubic form after annealing. This can save significantly both human and material resources when testing different dopants and dopant concentrations and avoiding the preparation of materials with the cubic form.

The DSC signal of the α - β transition was observed to broaden when the corresponding temperature rises. This may mean that there are various as-prepared products with

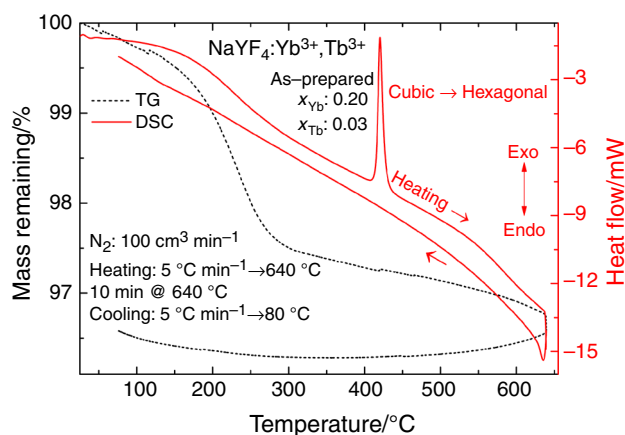
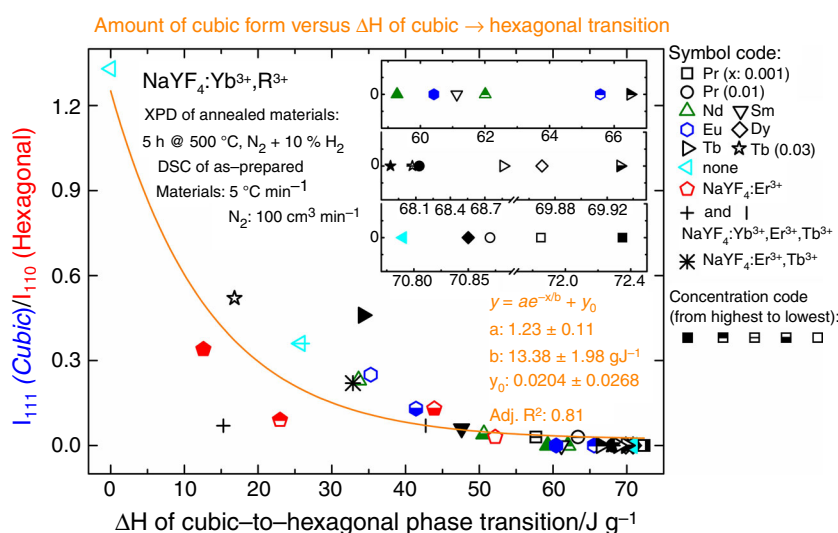


Fig. 5 TG and DSC curve of the $\text{NaYF}_4:\text{Yb}^{3+},\text{Tb}^{3+}$ material including also the cooling step

Fig. 4 Correlation between the intensity ratio of the 111 (cubic) and 110 (hexagonal form) reflections of the annealed $\text{NaYF}_4:\text{Yb}^{3+},\text{R}^{3+}$ (R: Pr, Nd, Sm, Eu, Tb, Dy or none) materials (from the XPD patterns) and the specific enthalpy of the cubic-to-hexagonal phase transition (DSC)



almost the same compositions and thus with slightly different transition temperatures. The experimental conditions such as the packing density and crystallite size of the material affect the signal width as well, but these parameters were not studied in this work.

The nature of the phase transitions was studied by measuring the DSC signal also during the cooling step (Fig. 5) because the high-temperature forms can be quenched to room temperature retaining their structures. DSC signals were not obtained in contrast to heating measurements. This indicates that the α - to β - NaRF_4 transition is irreversible, but the reason is not so clear though the generally better stoichiometry of the hexagonal phase is a plausible explanation. The absence of the signal for the HT cubic- β transition may be more easy to explain since the NaRF_4 composition starts to decompose (slowly) immediately above the β -HT cubic transition. As shown by the TG curve (Fig. 6), the $\text{NaRF}_4 \rightarrow \text{NaF(g)} + \text{RF}_3$ decomposition depletes the NaRF_4 phase of NaF and the HT-cubic- β reverse transition is then prevented. The phase transitions may thus depend on the exact stoichiometry of the material. And the other way round, such phase transitions may be triggered by changes in composition. The TG curves may offer a similar explanation to the α - β transition since a slight mass change can be found close to the phase transition temperature. This change is much less than the one at higher temperature but evidently enough to prevent the α - β transition to be reversible.

In addition to the mass changes around phase transitions, the TG curves of $\text{NaYF}_4:\text{Yb}^{3+},\text{R}^{3+}$ (R: Pr, Nd, Sm, Eu, Tb, Dy or none) showed a total mass loss of ca. 2–4 % during heating to 500 °C (Fig. 5), attributed mainly due to the removal of water, ethanol and possible crystal water (all below 300 °C). Only small mass changes were observed close to the chosen heating temperature (500 °C).

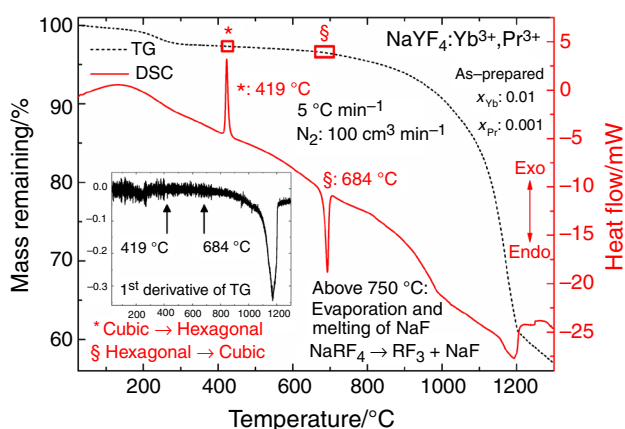


Fig. 6 DSC, TG and DTG curves of the $\text{NaYF}_4:\text{Yb}^{3+},\text{Pr}^{3+}$ material when heated up to 1300 °C

Up-conversion luminescence

With $\text{NaYF}_4:\text{Yb}^{3+},\text{R}^{3+}$ materials studied here, up-conversion luminescence was obtained from the following rare earths: Pr^{3+} , Nd^{3+} , Eu^{3+} , Tb^{3+} , Yb^{3+} and also from the Er^{3+} and Tm^{3+} impurities in the $\text{Y}^{3+}/\text{Yb}^{3+}$ precursor. Up-conversion luminescence was not obtained from Sm^{3+} and Dy^{3+} . The dopant concentrations with the strongest up-conversion luminescence varied significantly between Pr^{3+} and the other dopants: $x_{\text{Yb}}: 0.10 + x_{\text{R}}: 0.001$ (R: Pr^{3+}), $0.20 + 0.04$ (Nd^{3+}), $0.20 + 0.03$ (Eu^{3+}), $0.15 + 0.03$ (Tb^{3+}) and $0.20 + 0$ (none). The large difference in concentrations between Pr^{3+} and the other dopants, one order of magnitude, is due to, for example, cross-relaxation mechanisms. A detailed discussion on the up-conversion luminescence properties of the $\text{NaYF}_4:\text{Yb}^{3+},\text{R}^{3+}$ materials is out of scope of this work and will be published elsewhere in the future.

Up-conversion luminescence was observed of the Er^{3+} (and Tm^{3+}) impurities with several NaRF_4 materials because they are excited extremely effectively in the presence of the Yb^{3+} sensitizer [21, 23]. This should always be kept in mind because such impurities are common in the heavier rare earth oxide precursors due to the difficult separation of the heavier rare earths because of their very similar chemical properties. Er^{3+} emits at ca. 510–535, 535–565 and 630–685 nm due to the ${}^2\text{H}_{11/2}, {}^4\text{S}_{3/2}, {}^4\text{F}_{9/2} \rightarrow {}^4\text{I}_{15/2}$ transitions, respectively. Tm^{3+} emits at 460–485, 690–705 and 770–825 nm due to the ${}^1\text{G}_4, {}^3\text{F}_3, {}^3\text{H}_4 \rightarrow {}^3\text{H}_6$ transitions, respectively. All of these Er^{3+} and Tm^{3+} impurity emissions were observed from the $\text{NaYF}_4:\text{Yb}^{3+},\text{R}^{3+}$ materials—in many cases with or without the actual dopant.

Conclusions

The structure of the $\text{NaYF}_4:\text{Yb}^{3+},\text{R}^{3+}$ (R: Pr, Nd, Sm, Eu, Tb, Dy or none) materials studied was mainly hexagonal, but trace amounts of the cubic form were present in some materials, as well. The amount of the cubic form, the temperature of the α - to β - NaRF_4 transition and the specific enthalpy of this transition are intertwined. The rise in the temperature of the α - to β - NaRF_4 transition DSC signal indicates that the cubic-to-hexagonal change becomes more difficult requiring a higher temperature or more energy. If the DSC signal weakens at the same time (lower specific enthalpy), even a higher temperature does not help and the structure does not change, at least not completely, to hexagonal. The specific enthalpy of the transition is the key factor. It enables to estimate the amount of cubic form in annealed $\text{NaYF}_4:\text{Yb}^{3+},\text{R}^{3+}$ materials prior to the annealing, which can save time and work. However, the theoretical reason behind this connection is still unclear

and requires further studies, which will be carried out in the future. Finally, up-conversion luminescence was obtained of Pr³⁺, Nd³⁺, Eu³⁺, Tb³⁺, Er³⁺, and Tm³⁺ with the same Yb³⁺-doped NaYF₄ host.

Acknowledgements Financial support is acknowledged from the Nordic Energy Research (*AquaFEED* project), the Academy of Finland (projects *Energy Storage Luminophors 2* and *Novel Rare Earth Optical Sensors and Materials*—a bilateral project of Academy of Finland and CNPq, Brazil), the Graduate School of Materials Research (GSMR), as well as the University of Turku Graduate School (UTUGS), Turku, Finland.

References

- Auzel F. Upconversion and anti-stokes processes with f and d ions in solids. *Chem Rev.* 2004;104:139–73.
- Antal T, Harju E, Pihlgren L, Lastusaari M, Tyystjärvi T, Hölsä J, Tyystjärvi E. Use of near-infrared radiation for oxygenic photosynthesis via photon up-conversion. *Int J Hydrogen Energy.* 2012;37:8859–63.
- de Wild J, Meijerink A, Rath JK, van Stark WGJHM, Schropp REI. Upconverter solar cells: materials and applications. *Energy Environ Sci.* 2011;4:4835–48.
- Ylihärtilä M, Valta T, Karp M, Hattara L, Harju E, Hölsä J, Saviranta P, Waris M, Soukka T. Oligonucleotide array-in-well platform for detection and genotyping human adenoviruses by utilizing upconverting phosphor label technology. *Anal Chem.* 2011;83:1456–61.
- Krämer KW, Biner D, Frei G, Güdel HU, Hehlen M, Lüthi S. Hexagonal sodium yttrium fluoride based green and blue emitting upconversion phosphors. *Chem Mater.* 2004;16:1244–51.
- Zhao J, Sun Y, Kong X, Tian L, Wang Y, Tu L, Zhao J, Zhang H. Controlled synthesis, formation mechanism, and great enhancement of red upconversion luminescence of NaYF₄:Yb³⁺,Er³⁺ nanocrystals/submicroplates at low doping level. *J Phys Chem B.* 2008;112:15666–72.
- Hyppänen I, Hölsä J, Kankare J, Lastusaari M, Pihlgren L, Soukka T. Preparation and up-conversion luminescence properties of NaYF₄:Yb³⁺,Er³⁺ nanomaterials. *Terrae Rarae.* 2009;16:1–6.
- Harju E, Hyppänen I, Hölsä J, Kankare J, Lahtinen M, Lastusaari M, Pihlgren L, Soukka T. Polymorphism of NaYF₄:Yb³⁺,Er³⁺ up-conversion luminescence materials. *Z Kristallogr Proc.* 2011; 1:381–7.
- Thoma RE, Insley H, Hebert GM. Sodium fluoride–lanthanide trifluoride systems. *Inorg Chem.* 1966;5:1222–9.
- PCPDFWIN v. 1.30, Powder Diffraction File, 1997, International Centre for Diffraction Data, entries 06-0342 (cubic NaYF₄) and 28-1192 (hexagonal Na(Y_{0.57}Yb_{0.39}Er_{0.04})F₄).
- Mathews MD, Ambekar BR, Tyagi AK, Köhler J. *J Alloys Compd.* 2004;377:162–6.
- Malinowski M, Joubert M-F, Jacquier B. Infrared to blue up-conversion in Pr³⁺ doped YAG and LiYF crystals. *J Lumin.* 1994;60–61:179–82.
- Pollnau M, Hardman PJ, Clarkson WA, Hanna DC. Upconversion, lifetime quenching, and ground-state bleaching in Nd³⁺:LiYF₄. *Opt Commun.* 1998;147:203–11.
- Zhou Y, Lin J, Wang S. Energy transfer and upconversion luminescence properties of Y₂O₃:Sm and Gd₂O₃:Sm phosphors. *J Solid State Chem.* 2003;171:391–5.
- Stręk W, Dereń PJ, Bednarkiewicz A, Kalisky Y, Boulanger P. Efficient up-conversion in KYb_{0.8}Eu_{0.2}(WO₄)₂ crystal. *J Alloys Compd.* 2000;300–301:180–3.
- Stręk W, Bednarkiewicz A, Dereń PJ. Power dependence of luminescence of Tb³⁺-doped KYb(WO₄)₂ crystal. *J Lumin.* 2001;92:229–35.
- Wermuth M, Riedener T, Güdel HU. Spectroscopy and upconversion mechanisms of CsCdBr₃:Dy³⁺. *Phys Rev B.* 1998;57:4369–76.
- Müller P, Wermuth M, Güdel HU. Mechanisms of near-infrared to visible upconversion in CsCdBr₃:Ho³⁺. *Chem Phys Lett.* 1998;290:105–11.
- Yi G, Lu H, Zhao S, Ge Y, Yang W, Chen D, Guo LH. Synthesis, characterization, and biological application of size-controlled nanocrystalline NaYF₄:Yb,Er infrared-to-visible up-conversion phosphors. *Nano Lett.* 2004;4:2191–6.
- Heer S, Kömpe K, Güdel HU, Haase M. Highly efficient multi-colour upconversion emission in transparent colloids of lanthanide doped NaYF₄ nanocrystals. *Adv Mater.* 2004;16:2102–5.
- Hölsä J, Laihinne T, Laamanen T, Lastusaari M, Pihlgren L, Rodrigues LCV, Soukka T. Enhancement of the up-conversion luminescence from NaYF₄:Yb³⁺,Tb³⁺. *Phys B.* 2014;439:20–3.
- Geusic JE, Marcos HM, Van Uitert LG. Laser oscillations in Nd-doped yttrium aluminum, yttrium gallium and gadolinium garnets. *Appl Phys Lett.* 1964;4:182–4.
- Kaczmarek SM, Leniec G, Typek J, Boulon G, Bensalah A. Optical and EPR study of BaY₂F₈ single crystals doped with Yb. *J Lumin.* 2009;129:1568–74.